Molecular Pharmacology Fast Forward. Published on December 20, 2007 as doi:10.1124/mol.107.042101
This article has not been copyedited and formatted. The final version may differ from this version.

MOL #42101

MOLECULAR INTERACTIONS OF CCR5 WITH MAJOR CLASSES OF SMALL-MOLECULE ANTI HIV CCR5 ANTAGONISTS

Rama Kondru,* Jun Zhang, Changhua Ji, Tara Mirzadegan, David Rotstein, Surya Sankuratri and Marianna Dioszegi

Department of Medicinal Chemistry (RK, TM, DR) and Viral Diseases (MD, JZ, SS, CJ), Roche Palo Alto, 3431 Hillview Avenue, Palo Alto, CA 94304

Molecular Pharmacology Fast Forward. Published on December 20, 2007 as DOI: 10.1124/mol.107.042101
This article has not been copyedited and formatted. The final version may differ from this version.

Running Title: CCR5 Interactions with Small-Molecule Antagonists

Correspondence should be addressed to: Rama Kondru, Department of Medicinal Chemistry, Roche Palo Alto, 3431 Hillview Avenue, Palo Alto, CA 94304

Number of text pages: 32

Number of tables: 3

Number of figures: 10

Number of references: 39

Number of words in abstract: 185

Number of words in introduction: 729

Number of words in discussion: 1166

Abbreviations:

highly active anti-retroviral therapy (HAART); human immunodeficiency virus (HIV); extracellular loop (ECL); intracellular loop (ICL); maraviroc (MVC); aplaviroc (APL); vicriviroc (VVC); mean fluorescence intensity (MFI); cell-cell fusion (CCF); enfuvirtide (ENF); fluorescence-activated cell sorting (FACS); structure-activity relationship (SAR); G protein-coupled receptors (GPCR); transmembrane (TM)

Molecular Pharmacology Fast Forward. Published on December 20, 2007 as DOI: 10.1124/mol.107.042101
This article has not been copyedited and formatted. The final version may differ from this version.

Abstract

In addition to being an important receptor in leukocyte activation and mobilization, CCR5 is the essential coreceptor for human immunodeficiency virus (HIV). A large number of small molecule CCR5 antagonists have been reported that show potent activities in blocking chemokine function and HIV entry. To facilitate the design and development of next generation CCR5 antagonists, docking models for major classes of CCR5 antagonists were created by using site-directed mutagenesis and CCR5 homology modeling. Five clinical candidates: maraviroc, vicriviroc, aplaviroc, TAK-779 and TAK-220 were used to establish the nature of the binding pocket in CCR5. Although the five antagonists are very different in structure, shape and electrostatic potential, they were able to fit in the same binding pocket formed by the transmembrane (TM) domains of CCR5. Interestingly, each antagonist displayed a unique interaction profile with amino acids lining the pocket. Except for TAK-779, all antagonists showed strong interaction with Glu283 in TM 7 via their central basic nitrogen. The fully mapped binding pocket of CCR5 is being used for structure-based design and lead optimization of novel anti-HIV CCR5 inhibitors with improved potency and better resistance profile.

Molecular Pharmacology Fast Forward. Published on December 20, 2007 as DOI: 10.1124/mol.107.042101
This article has not been copyedited and formatted. The final version may differ from this version.

INTRODUCTION

Human immunodeficiency virus (HIV) enters the host cell via the interaction of the viral envelope protein gp160 and the receptor/coreceptors on host cell surface. The majority of primary HIV-1 strains use CCR5 as coreceptor (termed R5 virus), whereas some viruses are able to use another chemokine receptor, CXCR4, as coreceptor (termed X4 virus) or use both CCR5 and CXCR4 as coreceptors (termed R5X4 virus). Because CCR5 is the predominant coreceptor for clinical HIV isolates, and the normal physiology within the human genetic knockout population, CCR5 has become a very attractive target for anti-HIV therapy. A number of small molecule CCR5 antagonists have been identified that demonstrated potent anti-viral effects both in cell culture and in clinical trials.

TAK-779, a quaternary ammonium anilide, was the first small molecule CCR5 antagonist reported (Baba et al., 1999). This compound was terminated due to poor oral availability. Two structurally diverse followers TAK-220 and TAK-652 are both in clinical trials (Imamura et al., 2006; Seto et al., 2006). Several other small molecule CCR5 antagonists with good potency and/or pharmacological properties have also been reported by other pharmaceutical companies. These include SCH-C (SCH-351125), vicriviroc (VVC, SCH-D, SCH-417690), aplaviroc (APL, AK602, GW873140), and maraviroc (MVC, UK-427,857). SCH-C is an oximino-piperidino-piperidine amide (Palani et al., 2002) that showed potent antiviral activity in vivo. However, its clinical development was terminated due to HERG inhibitory activity. SCH-D is the next generation compound of SCH-C, which is in late stage clinical development. SCH-D showed better oral availability, potency, safety and pharmacological properties than SCH-C (Tagat et al., 2004). APL is a spirodiketopiperazine-based CCR5 antagonist that showed high antiviral potency and very slow receptor dissociation

Molecular Pharmacology Fast Forward. Published on December 20, 2007 as DOI: 10.1124/mol.107.042101
This article has not been copyedited and formatted. The final version may differ from this version.

(Maeda et al., 2004; Nakata et al., 2005). Clinical development of this compound was terminated in phase II/III due to liver toxicity (Crabb, 2006). MVC is a triazolotropane-based compound, and it is a small molecule CCR5 antagonist, currently marketed for the treatment of HIV. MVC demonstrated excellent antiviral potency and pharmacological properties (Dorr et al., 2005; Fatkenheuer et al., 2005; Wood and Armour, 2005).

All of these small molecule CCR5 inhibitors inhibit HIV-1 entry into target cells by blocking the interaction between gp120 and CCR5 (Dragic et al., 2000; Tsamis et al., 2003). Although the molecular mechanism of this activity is not clear, existing data suggests that antagonists inhibit viral entry through allosteric effects (Watson et al., 2005). The small molecule CCR5 antagonists sit in the pocket formed by the transmembrane (TM) domains of CCR5 (Dragic et al., 2000; Maeda et al., 2006; Nishikawa et al., 2005; Seibert et al., 2006; Tsamis et al., 2003) ; while HIV gp120 binds to the outer surface of CCR5, mainly by making contact with the N-terminus and the second extracellular loop (ECL) of CCR5 (Blanpain et al., 1999; Doranz et al., 1997; Dragic, 2001; Dragic et al., 1998; Farzan et al., 1998; Howard et al., 1999; Rabut et al., 1998; Ross et al., 1998; Rucker et al., 1996). Alanine scanning mutagenesis studies of CCR5 revealed several key residues required for the small molecule CCR5 antagonists to block HIV entry are located at the TM domains (Dragic et al., 2000; Maeda et al., 2006; Nishikawa et al., 2005; Seibert et al., 2006; Tsamis et al., 2003). These residues were identified by studying one or two classes of CCR5 antagonists. In order to gain a better view of the interaction between CCR5 antagonists and CCR5, studies were undertaken to understand the diversity of receptor interaction with representative advanced CCR5 antagonists. These CCR5 antagonists represent a variety of structure features (Fig. 1). Mutations that have been shown to affect antagonist-CCR5 interactions as well as some new mutations suggested by our homology modeling are included in the current study.

While all the antagonists share a common binding site, the nature of specific interactions within the pocket is rather unique to each of the molecules. Moreover, the extent of binding

Molecular Pharmacology Fast Forward. Published on December 20, 2007 as DOI: 10.1124/mol.107.042101
This article has not been copyedited and formatted. The final version may differ from this version.

derived from each of the pocket residues involved in ligand interaction is different for each of the antagonists. The binding modes developed using mutation data are further refined and validated using available structure-activity relationship (SAR) information. The sub-pockets are fully characterized for shape and electrostatic nature and a refined pharmacophore model for lead identification can be generated with ease. This fully mapped binding pocket for CCR5 has been effectively used as a structure-based design tool in the lead optimization of our own CCR5 antagonists.

MATERIALS AND METHODS

Reagents. All cell culture media and supplements and fetal bovine sera were purchased from Invitrogen (Carlsbad, CA). For CCR5 antagonists SCH-C (Palani et al., 2002), vicriviroc (VVC, SCH-D) (Strizki et al., 2005), Maraviroc (MVC, UK427,857) (Wood and Armour, 2005), aplaviroc (APL, GW873140, AK602) (Watson et al., 2005), TAK-779 (Baba et al., 1999) and TAK-220 (Imamura et al., 2006; Seto et al., 2006) please refer to their respective publications. The chemical names of the compounds are 4-[4-(1-Butyl-3-cyclohexylmethyl-2, 5-dioxo-1,4,9 triaza-spiro[5.5]undec-9-ylmethyl)-phenoxy]-benzoic acid (APL); 4,4-Difluoro-cyclohexanecarboxylic acid {(S)-3 [(1S,3S,5R)-3-(3-isopropyl-5-methyl-[1,2,4]triazol-4-yl)-8-aza-bicyclo[3.2.1]oct-8-yl]-1-phenyl-propyl}-amide (MVC); (4,6-Dimethyl-pyrimidin-5-yl)-(4-{(S)-4-[(R)-2 methoxy-1-(4-trifluoromethyl-phenyl)-ethyl]-3-methyl-piperazin-1-yl}-4-methyl-piperidin-1-yl)-methanone (VVC); Dimethyl-(tetrahydro-pyran-4-yl)-{4-[(3-p-tolyl-8,9-dihydro 7H-benzocycloheptene-6-carbonyl)-amino]-benzyl}-ammonium (TAK-779); 1-Acetyl-piperidine-4-carboxylic acid {3-[4-(4-carbamoyl-benzyl)-piperidin-1-yl]-propyl}-(3-chloro-4-methyl-phenyl)-amide (TAK-220); (4-{(4-Bromo-phenyl)-[(Z)-ethoxyimino]-methyl}-4'-methyl-[1,4']bipiperidinyl-1'-yl)-(2,4-dimethyl-1-oxy-pyridin-3-yl)-methanone (SCH-C).

Molecular Pharmacology Fast Forward. Published on December 20, 2007 as DOI: 10.1124/mol.107.042101
This article has not been copyedited and formatted. The final version may differ from this version.

Human CCR5 expression plasmid and mutagenesis. Human CCR5 (hCCR5) ORF was cloned by using polymerase chain reaction (PCR) from OriGene's TrueClone (Cat. No. TC110858, OriGene Technologies, Rockville, MD). The following PCR primers were used in reaction: 5'-primer, 5'-ATA-TAT-TAA-TCT-AGA-ACC-ATG-GAT-TAT-CAA-GTGTCA-AGT-C-3'; 3'-primer, 5'-ATA-TAT-TCT-AGA-GCG-GAT-CCT-CAC-AAG-CCC-ACA-GAT-ATT-TC-3'. The 1.1 kb PCR product was digested with *Xba*I and *BamH*I and cloned into mammalian expression vector pcDNA3.1(-) (Invitrogen, Carlsbad, CA). The clones were sequence confirmed and found to contain the identical human CCR5 coding sequence (GenBank Accession # NM_000579). Human CCR5 mutants were generated using the QuickChange Site-Directed Mutagenesis Kit (Stratagene, La Jolla, CA), following the protocol described by the manufacturer.

Stable expression of wild-type and mutant CCR5 in CHO-G16α cells. CHO-$G_{16\alpha}$ cells were transfected with plasmids carrying wild-type and mutant CCR5 by using the FuGene 6 (Roche Applied Science) transfection reagent, according to the manufacturer's instructions. Forty-eight hours after transfection, G418 was added to the medium to the final concentration of 1 mg/ml. Stable expression population of wild-type and mutant CCR5 was enriched by several rounds of fluorescence-activated cell sorting (FACS) using PE-labeled CCR5 mouse monoclonal antibody 2D7 (BD Pharmingen, San Diego, CA). Several CCR5 mutant failed to express on CHO-G16α cells. For those that were successfully expressed, the expression levels relative to the wild-type CCR5 were determined by FACS analysis.

Radioligand binding assays. ^{125}I-RANTES (regulated on activation normal T cell expressed and secreted), ^{125}I-MIP-1α (macrophage inflammatory protein-1α), and ^{125}I-MIP-1β were purchased from PerkinElmer Life Sciences Inc. (Shelton, CT). Binding assays were performed on CHO-hCCR5 whole cells as follows. Cells were plated in 96-well culture plates at 1.5 $\times 10^5$

Molecular Pharmacology Fast Forward. Published on December 20, 2007 as DOI: 10.1124/mol.107.042101
This article has not been copyedited and formatted. The final version may differ from this version.

cells/well in ice cold binding buffer (phenol red-free F12 medium supplemented with freshly made 0.1% BSA and 0.1% NaN_3). Serially diluted CCR5 inhibitors were added to the cells, followed by addition of 100 pM of the corresponding ^{125}I-labeled ligands. After 2 h of incubation at room temperature with gentle shaking, cells were harvested onto GF/C UniFilter plates (Perkin Elmer, Shelton, CT) using cell harvester. UniFilter plates were pretreated with 0.3% PEI /0.2% BSA for 30 min prior to harvest. Filter plates were washed 5 times with 25 mM pH 7.1 HEPES buffer containing 500 mM NaCl, 1 mM $CaCl_2$ and 5 mM $MgCl_2$. Plates were dried in 70^{o}C oven for 20 min and 40 µl scintillation fluid was added and radioactivity was measured using TopCount NXT (PerkinElmer, Shelton, CT). In all experiments, each data point was assayed in duplicate. Data are presented as the percentage of counts obtained in absence of cold competing ligand. Curve fitting and subsequent data analysis were carried out using GraphPad PRIZM software (Intuitive Software for Science, San Diego, Calif.) and IC_{50} values were calculated using non-linear regression analysis.

Cell-cell fusion assays.

Cell-based surrogate antiviral assay CCF assays were performed as described before (Ji et al., 2006). Briefly, Hela-R5 cells were plated in 384 well white culture plates (BD Bioscience, Palo Alto, CA) at 7.5 x 10^3 cells per well in phenol red-free Dulbecco's Modified Eagle Medium (DMEM) supplemented with 1 µg/ml Doxycycline. On the following day, serially diluted compounds were added to the plates followed by the addition of 1.5 x 10^4 cells/15 µl/well of CEM-NKr-CCR5luc target cells (NIH AIDS Research and Reference Reagent Program) and incubated overnight. At the end of co-culture, 15 µl of Steady-Glo luciferase substrate was added into each well, and the luciferase activity was measured.

Molecular Pharmacology Fast Forward. Published on December 20, 2007 as DOI: 10.1124/mol.107.042101
This article has not been copyedited and formatted. The final version may differ from this version.

Antiviral assay (Single-cycle HIV entry assay). The antiviral assay was performed as described before (Ji et al., 2006). Briefly, the equivalent of 1.5 x 10^5 RLU of Pseudotyped NL-Bal viruses was used to infect 2.5 x 10^4 JC53-BL cells (TZM-bl, NIH AIDS Research and Reference Reagent Program). After 3 day incubation at 37ºC, 50 µl of Steady-Glo Luciferase Assay System was added and the assay plates were read on a Luminometer (Luminsokan, Thermo Electron Corporation, Waltham, MA). IC_{50} was determined using the sigmoidal dose-response model with one binding site in Microsoft XLFit.

Computational methods. *(1) Sequence alignment.* The sequence alignment between bovine rhodopsin (1F88) and CCR5 was determined using the program Clustal W (Thompson et al., 1994). These sequence alignments were then imported into the MOE program [Molecular Operating Environment (Chemical Computing Group Inc., Montreal, Canada)] and were manually adjusted to improve the alignment of conserved residues in the trans-membrane regions. In general, most family A G protein-coupled receptors (GPCR) show a better homology in the TM regions compared to ECLs or intracellular loops (ICL). This is also true for CCR5, a better homology was identified within the TMs. There are two disulfide bridges in CCR5, one is between Cys101 and Cys178 and the other is between Cys20 and Cys269.

(2) Generation of the homology model using MOE. The sequence alignment (Fig. 2) was used to develop ten initial models using MOE. The homology model generation in MOE is a multi-step process. An initial geometry of CCR5 is generated using 1F88 (PDB code) as the template along with sequence alignments shown in Fig. 2. In the next step, ten CCR5 intermediate models are generated using the Boltzmann-weighted randomized modeling procedure (Levitt, 1992). The insertions and deletions within the structure are handled using the procedure described by Fechteler et al in 1995 (Fechteler et al., 1995). Loops are modeled following a contact energy function that analyzes the list of candidates taking into account all atoms already modeled. The coordinates for the loops are added using the Boltzmann-weighted

Molecular Pharmacology Fast Forward. Published on December 20, 2007 as DOI: 10.1124/mol.107.042101
This article has not been copyedited and formatted. The final version may differ from this version.

energy function. The side chain conformations are chosen from a rotamer library (Bower et al., 1997), and are further refined by energy minimization using CHARMM22 force field. After obtaining the structure of CCR5 from Rhodopsin, both the disulfide links were manually inserted between Cys20-Cys269 and Cys101-Cys178. Once the homology modeling procedure was finished, the final 10 models of CCR5 were individually inspected using MOE's stereochemical and conformational quality evaluation tools in order to confirm that the model's stereochemistry was reasonably consistent with typical values found in crystal structures. This was achieved by identification of outliers using Ramachandran plots (Morris et al., 1992). We analyzed multiple stereochemical and conformational parameters like omega angle, C-alpha chirality, chi angles and main chain bond angles and bond lengths and compared to values published in a statistical survey of high-resolution data in the Protein Data Bank (Laskowski et al., 1993) to determine outliers. All the non-bonded heavy atom clashes are removed by energy minimization of the final structure (Berman et al., 2000; Jones and Thirup, 1986).

(3) Identification of the putative binding pocket. A considerable cavity was found in the TM region of the receptor, in close proximity to the conserved E283 which was supposed to be one of the crucial residues for small molecule ligand binding in CCR5. The small molecules shown in Fig. 1 are basic in nature. This made us believe that the putative binding pocket is within the 6 Å vicinity of the critical residue E283. There is also lot of evidence in the literature suggesting a similar pocket for CCR2 (Mirzadegan et al., 2000) and other chemokine receptors. Some of the key residues within the putative binding pocket are W86, W94, Y108, F109, T195, I198, W248, Y251, E283 and M287 (Fig. 2). All these residues are individually mutated to alanine for studying their attribute in interaction with small molecule CCR5 antagonists shown in Fig. 2.

(4) Architecture of the antagonist binding site. The binding pocket of CCR5 is very hydrophobic with multiple aromatic residues lining the pocket. It is a very tight binding pocket. Based on the initial homology model it was clear that known CCR5 antagonists would not fit in

Molecular Pharmacology Fast Forward. Published on December 20, 2007 as DOI: 10.1124/mol.107.042101
This article has not been copyedited and formatted. The final version may differ from this version.

the pocket. Therefore, the side chain conformations had to be adjusted according to the size of the small molecule antagonists. Since residues W86, Y108, F109, T195, I198, W248, Y251 and E283 are in favorable positions to form the hydrophobic cavity, in all of our docking studies guided by CCR5 mutation data, we did not modify the backbone structure. We assumed that the backbone structure is conserved in all GPCRs. All the docking models for the antagonists are created by modifying the side chain conformations based on CCR5 mutagenesis study results. The modeled ECL2 is on top of the putative binding pocket as in Rhodopsin. CCR5 ECL2 and its role in the interaction with CCR5 antagonists were not considered for docking mainly due to high flexibility of the ECL2. The final antagonist docking model was obtained by relaxing all the amino acids within 6 Å of the ligand using the MMFF94x force field implemented in MOE.

RESULTS

CCR5 antagonists are potent inhibitors of ligand binding and HIV entry. Since the first report on the discovery of a potent CCR5 small molecule inhibitor TAK-779, a number of other structurally diverse CCR5 antagonists have been described. In order to understand the interactions between CCR5 and these CCR5 antagonists, five representative CCR5 antagonists were included in the current study. They are MVC, APL, VVC, TAK-779 and TAK-220 (Fig. 1.). All these compounds contain a basic nitrogen in the middle, but they possess different pharmacophoric features.

The antiviral and chemokine-blocking activities for these five antagonists are summarized in Table 1. All five small molecule inhibitors are potent CCR5 antagonists as demonstrated by their potent inhibition of the binding of the three natural ligands RANTES, MIP-1α and MIP-1β to CCR5. The Kd values for chemokines ^{125}I-RANTES, ^{125}I-MIP-1α and ^{125}I-MIP-1β binding to CCR5 are 0.59, 1.4, and 0.4 nM, respectively. VVC (Fig. 3A), MVC, and

Molecular Pharmacology Fast Forward. Published on December 20, 2007 as DOI: 10.1124/mol.107.042101
This article has not been copyedited and formatted. The final version may differ from this version.

TAK-779 inhibited the binding of all three ligands equally well. However, TAK-220 and APL showed distinct inhibition profiles. TAK-220 potently inhibited the binding of RANTES and MIP-1α, yet it barely inhibited the binding of MIP-1β. While in the case of APL, it potently inhibited the binding of MIP-1α and MIP-1β, but it only partially inhibited the binding of RANTES, with a maximal inhibition of about 70% (Fig. 3B). This is consistent with previously published results (Watson et al., 2005). These results suggest that although these antagonists may share a common binding site, they may not exert the same allosteric effects on the receptor.

Because these CCR5 antagonists are mainly developed for antiviral indication, it is important to determine if the ligand displacement activity is correlated with the antiviral activity. As shown in Table 1, all five antagonists are also potent inhibitors of HIV entry as assessed in two different HIV entry assays: CCF assay and single-cycle HIV entry assay. It is noteworthy that although the ligand binding inhibition is generally correlated with HIV entry inhibition, better correlation was found between the two HIV entry assays. Nevertheless, the good correlation of chemokine antagonism and viral entry inhibition validates the use of ligand binding assays for the current study.

Shape and Electrostatic nature of the CCR5 antagonists. Interestingly, the compounds APL, MVC, VVC, TAK-779, and TAK-220 are very different in shape and electrostatic potential, although they share the same binding pocket (Fig. 5). The conformational analysis showed that the conformational space accessed by these compounds is very different. The proposed active conformation resulting from docking was used to generate the electrostatic potential maps. Our hypothesis is that the CCR5 receptor is able to accommodate these structurally and electrostatically diverse antagonists by utilizing a unique set of interactions for every ligand. The electrostatic surface colored using the active lone pairs for all five antagonists is shown in Fig. 5. The polar atoms are indicated by pink colored grid; and the electropositive aromatic ring

Molecular Pharmacology Fast Forward. Published on December 20, 2007 as DOI: 10.1124/mol.107.042101
This article has not been copyedited and formatted. The final version may differ from this version.

hydrogen atoms are shown in blue; the green regions highlight the hydrophobic surface of the molecules.

CCR5 antagonists interact with a pocket formed by the TM helices**.** It is believed that all GPCR share an overall common structure, and all have a pocket formed by the TM helices. Small molecule compounds may sit in the pocket (similar to retinal binding in Rhodopsin) and may serve as an agonist or an antagonist. Previously published data suggest that CCR5 antagonists also bind to this conserved pocket (Maeda et al., 2006). By using homology modeling, a putative binding site in CCR5 was defined, and the residues that surround the traditional small molecule binding pocket are identified. The putative binding site is towards the extracelluar side of CCR5 between transmembrane helices (I-VII). Similar binding pockets have been previously described in the literature for other chemokine receptors. Nine of the surrounding residues are shown in Fig. 4. In order to evaluate the potential interactions of these residues with the antagonists, each of these amino acid residues was mutated to alanine in the wild-type CCR5. The wild-type and individual mutant CCR5 that carries a single residue mutation were stably expressed in CHO cells and influence of various CCR5 antagonists on ^{125}I-RANTES binding was measured on these cells.

All CCR5 mutant stable cell lines were monitored for expression by FACS and their expression levels differ from that of the wild-type CCR5 within two-fold (Table 2). Five of the mutations T195A, I198A, W248A, Y251 and M287A did not significantly change the binding affinity of RANTES to CCR5; however, mutation W86A, F109A and E283A reduced the binding affinity of RANTES to CCR5 by 5, 10, and 20 fold, respectively (Table 2). The Kd values of RANTES for two CCR5 mutants W94A and Y108A were not determined because no saturation of CCR5 was observed within the studied concentration range. IC_{50} values for CCR5 antagonists in inhibiting RANTES binding to the wild-type CCR5 and various mutants were then

Molecular Pharmacology Fast Forward. Published on December 20, 2007 as DOI: 10.1124/mol.107.042101
This article has not been copyedited and formatted. The final version may differ from this version.

measured and summarized in Table 2. The inhibition curves of the 5 antagonists on RANTES binding to the wild-type and E283A mutant CCR5 were shown in Fig. 3C & D. All five antagonists exhibited lower RANTES displacement potency in most of the CCR5 mutants. To facilitate the visualization of the changes in antagonists binding to various CCR5 mutants, IC_{50} fold changes were calculated for each mutant and each compound and these data are summarized in Table 3. Except in the case of TAK-220 which slightly gained binding to CCR5 T195A, Y108A, F109A, Y251A, or W248A mutants, all other antagonists showed reduced binding affinity to CCR5 carrying single amino acid mutations. No two antagonists showed similar binding profile against these mutants, and each mutation had a varying degree of effect on the binding of the five antagonists. For example, while CCR5 mutation F109A had no significant impact on MVC binding (IC_{50} fold change = 0.9), it significantly reduced APL binding to CCR5 (IC_{50} fold change = 158). Among all the mutants studied, E283A exhibited the greatest impact on the binding of antagonists MVC, VVC, and TAK-220. TAK-779 binding to CCR5 was only significantly affected by two mutations W86A and Y108A (53 and 28 fold loss in binding respectively), and it was weakly affected by E283A mutation (11 fold reduction in binding). However, E283A caused significant loss (61 – 2000 fold) of binding of the other 4 antagonists. This may be explained by the fact that TAK-799 is structurally most diverse from the other four antagonists. A single mutation that caused the maximal loss of APL binding to CCR5 is F109A (158 fold), although E283A also markedly affected APL binding (61 fold). Mutations W94A and M287A showed no significant effects and T195A, W248A and Y251A showed only moderate effects on the binding of these five CCR5 antagonists (Table 2 & 3). The mutation data were used for building the binding modes for the five CCR5 antagonists APL, MVC, VVC, TAK-779 and TAK-220.

APL binding mode. One of the key interactions for the compounds that contain a basic nitrogen (APL, MVC, VVC, SCH-C, TAK-220) is with E283. The strength of this interaction varies

Molecular Pharmacology Fast Forward. Published on December 20, 2007 as DOI: 10.1124/mol.107.042101
This article has not been copyedited and formatted. The final version may differ from this version.

among the compounds we studied, strongest interaction with E283 was seen for MVC and the weakest interaction was found for TAK-779. Two aromatic side chains F109 and W86 are predicted to interact with APL (Fig. 6). This is consistent with the mutant profile shown in Table 3 that APL lost binding to CCR5 mutant W86A by 39 fold. The fold loss for SCH-C is 264 (data not shown) indicating that SCH-C interacts much more strongly with W86 than APL. By comparing fold losses between various compounds for a single mutation, we could identify the range of interaction strength for each residue. For example, W86A mutation resulted in a marginal 1.8-fold binding reduction for TAK-220 yet a large 264-fold binding reduction for SCH-C. This implies that TAK-220 interacts weakly with W86. These comparative results are utilized for prioritization of docking processes when there are multiple choices for binding modes. Additionally, we predict a weak interaction with E283 as compared to other compounds we profiled. The polar residue T195 has a hydrogen bond with the hydroxyl group on APL, this is clearly manifested in the mutant profile with 12 fold loss when T195 is mutated to an alanine. This particular H-bond interaction is the strongest with APL as compared to others. The cyclohexyl end of the APL structure is predicted to interact with I198. There is a 35 fold loss in the I198A mutant, this is clearly one of the strongest hydrophobic interactions. The aromatic residues Y108, W248 and Y251 show the weakest interaction with a flat mutant profile. There could be multiple reasons why these residues that are predicted to be in the vicinity of the binding pocket do not show strong interactions with APL. We hypothesize that the mutation of one of these aromatic residues may cause others to collapse into the binding pocket without altering the overall IC_{50}. This kind of hydrophobic collapse may suggest that placing flexible linkers for CCR5 antagonists in this region between TM5 and TM6 could be well tolerated. The t-butyl of APL is buried within the helical bundle via strong hydrophobic interactions with multiple aromatic residues. Overall, the key interactions for APL are with W86 on TM2, Phe109 on TM3, I198 on YM5, and E283 on TM7.

Molecular Pharmacology Fast Forward. Published on December 20, 2007 as DOI: 10.1124/mol.107.042101
This article has not been copyedited and formatted. The final version may differ from this version.

MVC binding mode. The strongest interactions are predicted between MVC and glutamic acid E283 (Fig. 7). In the E283A mutant MVC showed a 2000-fold loss in RANTES displacement potency. This is a strong salt-bridge interaction. The strength of salt-bridge interactions decreases sharply if the distance between the interacting groups increases. This is due to the distance dependence of the salt-bridge interaction as well as the strong desolvation for charged amines. The aromatic interaction with W86 for MVC involves T-shaped π–π stacking while the interaction with Phe109 is predicted to be mainly hydrophobic in nature. The Y108A mutation resulted in a 70-fold loss of MVC binding ability. Y108 is predicted to interact with the phenyl ring on MVC via a parallel displaced interaction. The amide connected to the difluoro-cyclohexyl group is not part of any key interactions. We propose that this amide linker is used as a conformational constraint for the placement of the difluorocyclohexyl group. Binding of MVC to CCR5 was also markedly reduced in the I198A CCR5 mutant. The interaction between MVC and I198 is predicted to be primarily hydrophobic in nature. The interaction of MVC with Y251 is only moderate with a mere 12.2-fold reduction in binding to the Y251A mutant. However, all the compounds profiled in this study showed a small degree of change when Y251 is mutated to alanine. It is hypothesized that Y251 is flexible enough to move in and out of the binding pocket depending on the compound size and electrostatic nature. The W86 residue interacts weakly with MVC as compared to APL. We think that suboptimal placement of the triazole group of MVC may be the reason. In summary, the key residues involved in the interactions with MVC are E283 on TM7, Y108 on TM3, I198 on TM5, and Y251 on TM6.

VVC binding mode. The interaction strengths deciphered from mutation data were also used to develop the docking mode for VVC (Fig. 8). The trifluoromethyl phenyl group in VVC is predicted to interact strongly with I198 via hydrophobic interactions. This phenyl group also interacts with Y108 via an edge-to-face (T shaped) aromatic staked interaction. This T shaped edge-to-face aromatic interaction is critical for VVC binding to CCR5 because I198A mutation

Molecular Pharmacology Fast Forward. Published on December 20, 2007 as DOI: 10.1124/mol.107.042101
This article has not been copyedited and formatted. The final version may differ from this version.

caused 60-fold loss in binding. The trifluoromethyl phenyl group of VVC occupies a pocket with large volume. Additional groups may be tolerated in this large volume surrounded by several residues on TM3, TM5 and TM6. The hydrophilic volume within the central core of the pocket between TM3 and TM7 is occupied by the quaternary nitrogen. The 700-fold loss in VVC binding to CCR5 E283A mutant may be explained by stronger electrostatic interactions between the positively charged tertiary nitrogen group of VVC and the hydrophilic region contributed by E283. This is consistent with the proximity of the basic group of VVC and hydrophilic region predicted from our docking results. The contributions of T195 on TM5, W86 and W96 on TM2, F109 on TM3, W248 on TM6, and M287 on TM7 to VVC binding is considered minimal. However, the interaction with Y251 is substantial and it is the strongest for VVC compared to other compounds profiled in this study. Overall, the key interactions of VVC are predicted to be with Y108 on TM3, Y251 on TM6, E283 on TM7, and I198 on TM5.

TAK-779 binding mode. Multiple interactions are predicted between TAK-779 and two aromatic side chains of Y108 and W86. Y108 is predicted to interact via T-shaped π–π stacking with phenyl group of the bicyclic ring on TAK-779 (Fig. 9). There are additional interactions with T195, I198, F109, W248 and Y251. While these interactions are not strong, as suggested by the mutation data, they offer a large number of contacts that are hydrophobic in nature. Also, one can assume that when residues in such close proximity to the pocket are mutated individually, depending on the antagonists shape and size, other residues can move in to form the hydrophobic shell. This phenomenon will lead to a smaller degree of change in IC_{50} values for TAK-779. Several cases that mutation of residues directly in contact with the ligand resulted in a small effect on binding and/or activity have been reported in the literature. This is due to hydrophobic collapse resulting in a pocket of similar size and hydrophobic nature when some residues are mutated. The hydrophilic volume represented by E283 is not properly utilized by TAK-779. The quaternary ammonium ion does not use the interaction with E283 adequately. This could be due

Molecular Pharmacology Fast Forward. Published on December 20, 2007 as DOI: 10.1124/mol.107.042101
This article has not been copyedited and formatted. The final version may differ from this version.

to the increased salt bridge distance caused by methyl groups shielding the positive charge. This is evident from the fact that the E283A mutant resulted in a mere 11-fold loss in binding for TAK-779. It is interesting to note that of all the compounds studied, TAK-779 was least affected by E283A mutation. The para-methyl phenyl group on TAK-779 is predicted to interact strongly with I198 on TM5. Overall, TAK-779 was found to have strong interactions with W86 on TM2 and Y108 on TM3 and weak interaction with E283. There are also several weak hydrophobic interactions with T195 on TM5, I198 on TM5, F109 on TM3, W248 and Y251 on TM6.

TAK-220 binding mode.

TAK-220 is a conformationally flexible molecule with multiple rotatable bonds. It also displayed a unique CCR5 mutant binding profile, when compared with other compounds profiled in this study. Two mutations (E283A and I198A) resulted in significant reduction in TAK-220 binding while other mutations did not have any effect on TAK-220 binding to CCR5 (Fig. 10). This may be explained by the high flexibility of TAK-220 conformation.. The observed loss in binding (647 fold) to the CCR5 E283A mutant suggested a strong salt-bridge interaction between E283 and TAK-220. The other strong interaction of TAK-220 with CCR5 is predicted to be the hydrophobic interaction with I198. The mutations at residues W86, Y108, W248, Y251, T195 and M287 showed surprisingly little effects on TAK-220 binding. This could be due to hydrophobic collapse of the residues within the pocket around TAK-220. When there is a hydrophobic collapse, the individual interactions between various atom types within the pocket may be weak, but the combined interactions are strong. It was difficult to define the binding mode for TAK-220 just based on the CCR5 mutation data. Docking modes developed for other molecules were also used to guide the docking process for TAK-220. There are structural features that TAK-220 shares with MVC, which became evident when these two compounds were overlayed within the pocket. For example, a 3-chloro-4-methyl phenyl group of TAK-220 is placed in the similar region within the helical bundle as the phenyl group of MVC. The TAK-

Molecular Pharmacology Fast Forward. Published on December 20, 2007 as DOI: 10.1124/mol.107.042101
This article has not been copyedited and formatted. The final version may differ from this version.

220 binding mode developed this way predicts that additional interactions with CCR5 exist at positions F109, W248 and Y251 within the helical bundle (Fig. 10). Although these interactions are not strong individually as suggested by the mutation data, they may be significant enough for binding in combination since all of them are hydrophobic in nature.

DISCUSSION

In the current study, a putative binding pocket was defined and five small molecule CCR5 antagonists representing all main structural classes were modeled for their interaction with CCR5. All important residues surrounding the binding pocket were mutated for the investigation of their roles in interacting with the compounds. To date this report is the most comprehensive study on CCR5-antagonists interaction modeling.

Similar studies have been published before to characterize molecular interactions between CCR5 antagonists and CCR5. However, majority of these studies only focused on one or two classes of small molecule CCR5 inhibitors. (Dragic et al., 2000; Nishikawa et al., 2005; Seibert et al., 2006; Tsamis et al., 2003). For example, TAK-779 is the only CCR5 antagonist used in the first reported CCR5 mutagenesis study (Dragic et al., 2000) and in the next similar study SCH-C and AD101 that belongs to the same structure class were evaluated (Tsamis et al., 2003). In two other studies, either TAK-220 (Nishikawa et al., 2005) or TAK-779 (Seibert et al., 2006) was investigated along with Schering-Plough CCR5 inhibitors. Furthermore, none of these studies included the only marketed CCR5 antagonist MVC and the other clinically most advanced CCR5 antagonist VVC. VVC is structurally very similar to AD101 and SCH-C, however, overlapping but different resistance mutation profiles have been found for VVC and AD101 (Marozsan et al., 2005), suggesting they may interact with CCR5 differently. This is also supported by the observation that the closely related inhibitors AD101 and SCH-C interact with different sites on CCR5 (Tsamis et al., 2003). Therefore, characterizing the binding sites on

CCR5 for VVC and MVC are of great importance. The classes of compounds chosen here are the ones reached clinical trials or approved for clinical use. In addition, different assay systems were used in the previously published CCR5 antagonist-receptor interaction studies, results from different assays may not necessarily be comparable (Dragic et al., 2000; Maeda et al., 2006; Seibert et al., 2006). Hence it is very important to analyze the molecular interactions for all antagonists under the same assay conditions and using the same set of CCR5 mutations. Although results from the current study are generally in line with published data, several new key observations have been made. For instance, the important interactions for APL have been previously mapped to Y108, G163, K191, I198, Y251 and E283 (Maeda et al., 2006), in the current study, two additional critical interacting residues were identified (W86, and F109), and Y251 turned out to be an unimportant residue for APL antagonism. While SCH-C and TAK-779 have been previously shown to bind to similar sites (Maeda et al., 2006), our results suggest that SCH-C and VVC bind to significantly different sets of residues from TAK-779.

Although all antagonists bind to the same hydrophobic pocket in CCR5, they occupy different sub-cavities. This is clearly demonstrated by their different CCR5 mutant binding profiles. This is in agreement with their significantly different electrostatic shapes and polarities. All antagonists seem to share certain interactions such as with residue E283. However, the primary interaction residues for every antagonist were found to be different. The range of electrostatic salt-bridge interactions with E283 vary with the ligand and is not correlated to the basicity of the amine, but to the position of this positively charged amine within the pocket relative to the acidic E283 residue. It appears that two sets of interactions exist for each molecule: the primary set of interactions that are critical for binding and the secondary set that collapses after the primary set. Both sets of interactions are compound-dependent. To our surprise, I198 plays an important role in the binding of VVC, MVC, APL, and TAK-220, since it is such a small residue. Our CCR5 mutant binding data suggests that a few residues including hydrophobic residues (M287, W94 and W248) surrounding the binding pocket were not as

important for the binding of these five tested antagonists. This may suggest that these residues were not properly positioned for the small molecule antagonists to use, or the antagonists could make adjustment when each of them was mutated to alanine. Other antagonists that were not examined in this study, however, may use these residues for interaction with CCR5. It is also interesting to observe that mutations of certain residues to alanine resulted in better RANTES displacement activities of some antagonists. For instance, TAK-220 binds to CCR5 mutant T195A, F109A and W248A slightly better than to the wild-type CCR5 (Table 3). According to our model, Y108 adapts two different conformations with TAK-779 and VVC. Similarly, W86 changes conformation when interacting with MVC and TAK-779. In addition, knowledge derived from the binding mode of one compound can be used for the modeling of other antagonists. The development of TAK-220 binding mode utilized the binding mode of MVC. In fact, the binding modes of these standards CCR5 antagonists were routinely used for guiding the design of our novel CCR5 inhibitors. Information on structure elements of the compounds and their interaction with specific residues on CCR5 could be applied to the construction of new and more potent small molecule CCR5 antagonists.

Published and our results suggest that CCR5 antagonists sit in the pocket formed by the TMs through interactions with different sets of residues primarily located in the TM regions. It has been suggested that these small molecule antagonists inhibit chemokine ligand binding in a non-competitive manner (Watson et al., 2005). In addition, the inhibition of HIV entry by CCR5 antagonits is by allosteric mechanism. It has been reported that MVC-resistant HIV mutants can bind to the receptor while MVC is bound to the transmemebrane domains of the CCR5, suggesting that the viral binding site and antagonist binding site are independent and the inhibition of viral entry is by allosteric mechanism (Westby et al., 2007). However, the mechanism of allosteric inhibition is not fully understood yet. Allosteric antagonism could be achieved by inducing conformational changes in CCR5 or stabilizing different possible conformation states of unoccupied receptor. It is highly likely that CCR5 antagonists can induce

Molecular Pharmacology Fast Forward. Published on December 20, 2007 as DOI: 10.1124/mol.107.042101
This article has not been copyedited and formatted. The final version may differ from this version.

conformational changes in CCR5, and these changes can be very complex and involve multiple steps and multiple conformation states. Interestingly, it was reported that APL allows RANTES to bind to CCR5 yet it prevents RANTES triggered CCR5 activation (Watson et al., 2005).

To facilitate the design and development of next generation CCR5 antagonists, docking models for major classes of CCR5 antagonists were created by using site-directed mutagenesis and CCR5 homology modeling. Five clinical candidates: maraviroc, vicriviroc, aplaviroc, TAK-779 and TAK-220 were used to establish the nature of the binding pocket in CCR5. The structure, shape and electrostatic differences and their binding modes could be exploited to identify opportunities for design of new and novel compounds. Even the unique interaction profile with amino acids lining the pocket for various antagonists could also help in developing new compounds with no cross resistance to first generation CCR5 antagonists for HIV. The fully mapped binding pocket of CCR5 is been used for structure-based design and lead optimization of novel CCR5 antagonists.

ACKNOWLEDGEMENTS

The authors would like to acknowledge medicinal chemists Richard Cournoyer, Ferenc Makra, and Lubov Filonova at Roche Palo Alto for their assistance. We also like to thank our colleagues in the HIV Biology Group at Roche Palo Alto for providing the single-cycle HIV entry data for the five antagonists used in this paper.

REFERENCES

Baba M, Nishimura O, Kanzaki N, Okamoto M, Sawada H, Iizawa Y, Shiraishi M, Aramaki Y, Okonogi K, Ogawa Y, Meguro K and Fujino M (1999) A small-molecule, nonpeptide CCR5 antagonist with highly potent and selective anti-HIV-1 activity. *Proc Natl Acad Sci U S A* **96**:5698-703.

Berman HM, Westbrook J, Feng Z, Gilliland G, Bhat TN, Weissig H, Shindyalov IN and Bourne PE (2000) The Protein Data Bank. *Nucleic Acids Res* **28**:235-42.

Blanpain C, Doranz BJ, Vakili J, Rucker J, Govaerts C, Baik SS, Lorthioir O, Migeotte I, Libert F, Baleux F, Vassart G, Doms RW and Parmentier M (1999) Multiple charged and aromatic residues in CCR5 amino-terminal domain are involved in high affinity binding of both chemokines and HIV-1 Env protein. *J Biol Chem* **274**:34719-27.

Bower MJ, Cohen FE and Dunbrack RL, Jr. (1997) Prediction of protein side-chain rotamers from a backbone-dependent rotamer library: a new homology modeling tool. *J Mol Biol* **267**:1268-82.

Crabb C (2006) GlaxoSmithKline ends aplaviroc trials. *Aids* **20**:641.

Doranz BJ, Lu ZH, Rucker J, Zhang TY, Sharron M, Cen YH, Wang ZX, Guo HH, Du JG, Accavitti MA, Doms RW and Peiper SC (1997) Two distinct CCR5 domains can mediate coreceptor usage by human immunodeficiency virus type 1. *J Virol* **71**:6305-14.

Dorr P, Westby M, Dobbs S, Griffin P, Irvine B, Macartney M, Mori J, Rickett G, Smith-Burchnell C, Napier C, Webster R, Armour D, Price D, Stammen B, Wood A and Perros M (2005) Maraviroc (UK-427,857), a potent, orally bioavailable, and selective small-molecule inhibitor of chemokine receptor CCR5 with broad-spectrum anti-human immunodeficiency virus type 1 activity. *Antimicrob Agents Chemother* **49**:4721-32.

Dragic T (2001) An overview of the determinants of CCR5 and CXCR4 co-receptor function. *J Gen Virol* **82**:1807-14.

Dragic T, Trkola A, Lin SW, Nagashima KA, Kajumo F, Zhao L, Olson WC, Wu L, Mackay CR, Allaway GP, Sakmar TP, Moore JP and Maddon PJ (1998) Amino-terminal substitutions in the CCR5 coreceptor impair gp120 binding and human immunodeficiency virus type 1 entry. *J Virol* **72**:279-85.

Dragic T, Trkola A, Thompson DA, Cormier EG, Kajumo FA, Maxwell E, Lin SW, Ying W, Smith SO, Sakmar TP and Moore JP (2000) A binding pocket for a small molecule inhibitor of HIV-1 entry within the transmembrane helices of CCR5. *Proc Natl Acad Sci U S A* **97**:5639-44.

Farzan M, Choe H, Vaca L, Martin K, Sun Y, Desjardins E, Ruffing N, Wu L, Wyatt R, Gerard N, Gerard C and Sodroski J (1998) A tyrosine-rich region in the N terminus of CCR5 is important for human immunodeficiency virus type 1 entry and mediates an association between gp120 and CCR5. *J Virol* **72**:1160-4.

Fatkenheuer G, Pozniak AL, Johnson MA, Plettenberg A, Staszewski S, Hoepelman AI, Saag MS, Goebel FD, Rockstroh JK, Dezube BJ, Jenkins TM, Medhurst C, Sullivan JF, Ridgway C, Abel S, James IT, Youle M and van der Ryst E (2005) Efficacy of short-term monotherapy with maraviroc, a new CCR5 antagonist, in patients infected with HIV-1. *Nat Med* **11**:1170-2.

Fechteler T, Dengler U and Schomburg D (1995) Prediction of protein three-dimensional structures in insertion and deletion regions: a procedure for searching data bases of representative protein fragments using geometric scoring criteria. *J Mol Biol* **253**:114-31.

Howard OM, Shirakawa AK, Turpin JA, Maynard A, Tobin GJ, Carrington M, Oppenheim JJ and Dean M (1999) Naturally occurring CCR5 extracellular and transmembrane domain variants affect HIV-1 Co-receptor and ligand binding function. *J Biol Chem* **274**:16228-34.

Imamura S, Ichikawa T, Nishikawa Y, Kanzaki N, Takashima K, Niwa S, Iizawa Y, Baba M and Sugihara Y (2006) Discovery of a piperidine-4-carboxamide CCR5 antagonist (TAK-220) with highly potent Anti-HIV-1 activity. *J Med Chem* **49**:2784-93.

Ji C, Zhang J, Cammack N and Sankuratri S (2006) Development of a novel dual CCR5-dependent and CXCR4-dependent cell-cell fusion assay system with inducible gp160 expression. *J Biomol Screen* **11**:65-74.

Jones TA and Thirup S (1986) Using known substructures in protein model building and crystallography. *Embo J* **5**:819-22.

Laskowski RA, Moss DS and Thornton JM (1993) Main-chain bond lengths and bond angles in protein structures. *J Mol Biol* **231**:1049-67.

Levitt M (1992) Accurate modeling of protein conformation by automatic segment matching. *J Mol Biol* **226**:507-33.

Maeda K, Das D, Ogata-Aoki H, Nakata H, Miyakawa T, Tojo Y, Norman R, Takaoka Y, Ding J, Arnold GF, Arnold E and Mitsuya H (2006) Structural and molecular interactions of CCR5 inhibitors with CCR5. *J Biol Chem* **281**:12688-98.

Maeda K, Nakata H, Koh Y, Miyakawa T, Ogata H, Takaoka Y, Shibayama S, Sagawa K, Fukushima D, Moravek J, Koyanagi Y and Mitsuya H (2004) Spirodiketopiperazine-based CCR5 inhibitor which preserves CC-chemokine/CCR5 interactions and exerts potent activity against R5 human immunodeficiency virus type 1 in vitro. *J Virol* **78**:8654-62.

Marozsan AJ, Kuhmann SE, Morgan T, Herrera C, Rivera-Troche E, Xu S, Baroudy BM, Strizki J and Moore JP (2005) Generation and properties of a human immunodeficiency virus type 1 isolate resistant to the small molecule CCR5 inhibitor, SCH-417690 (SCH-D). *Virology* **338**:182-99.

Mirzadegan T, Diehl F, Ebi B, Bhakta S, Polsky I, McCarley D, Mulkins M, Weatherhead GS, Lapierre JM, Dankwardt J, Morgans D, Jr., Wilhelm R and Jarnagin K (2000) Identification of the binding site for a novel class of CCR2b chemokine receptor antagonists: binding to a common chemokine receptor motif within the helical bundle. *J Biol Chem* **275**:25562-71.

Morris AL, MacArthur MW, Hutchinson EG and Thornton JM (1992) Stereochemical quality of protein structure coordinates. *Proteins* **12**:345-64.

Nakata H, Maeda K, Miyakawa T, Shibayama S, Matsuo M, Takaoka Y, Ito M, Koyanagi Y and Mitsuya H (2005) Potent anti-R5 human immunodeficiency virus type 1 effects of a CCR5 antagonist, AK602/ONO4128/GW873140, in a novel human peripheral blood mononuclear cell nonobese diabetic-SCID, interleukin-2 receptor gamma-chain-knocked-out AIDS mouse model. *J Virol* **79**:2087-96.

Nishikawa M, Takashima K, Nishi T, Furuta RA, Kanzaki N, Yamamoto Y and Fujisawa J (2005) Analysis of binding sites for the new small-molecule CCR5 antagonist TAK-220 on human CCR5. *Antimicrob Agents Chemother* **49**:4708-15.

Palani A, Shapiro S, Josien H, Bara T, Clader JW, Greenlee WJ, Cox K, Strizki JM and Baroudy BM (2002) Synthesis, SAR, and biological evaluation of oximino-piperidino-piperidine amides. 1. Orally bioavailable CCR5 receptor antagonists with potent anti-HIV activity. *J Med Chem* **45**:3143-60.

Rabut GE, Konner JA, Kajumo F, Moore JP and Dragic T (1998) Alanine substitutions of polar and nonpolar residues in the amino-terminal domain of CCR5 differently impair entry of macrophage- and dualtropic isolates of human immunodeficiency virus type 1. *J Virol* **72**:3464-8.

Ross TM, Bieniasz PD and Cullen BR (1998) Multiple residues contribute to the inability of murine CCR-5 to function as a coreceptor for macrophage-tropic human immunodeficiency virus type 1 isolates. *J Virol* **72**:1918-24.

Rucker J, Samson M, Doranz BJ, Libert F, Berson JF, Yi Y, Smyth RJ, Collman RG, Broder CC, Vassart G, Doms RW and Parmentier M (1996) Regions in beta-chemokine receptors CCR5 and CCR2b that determine HIV-1 cofactor specificity. *Cell* **87**:437-46.

Seibert C, Ying W, Gavrilov S, Tsamis F, Kuhmann SE, Palani A, Tagat JR, Clader JW, McCombie SW, Baroudy BM, Smith SO, Dragic T, Moore JP and Sakmar TP (2006) Interaction of small molecule inhibitors of HIV-1 entry with CCR5. *Virology* **349**:41-54.

Seto M, Aikawa K, Miyamoto N, Aramaki Y, Kanzaki N, Takashima K, Kuze Y, Iizawa Y, Baba M and Shiraishi M (2006) Highly potent and orally active CCR5 antagonists as anti-HIV-1 agents: synthesis and biological activities of 1-benzazocine derivatives containing a sulfoxide moiety. *J Med Chem* **49**:2037-48.

Strizki JM, Tremblay C, Xu S, Wojcik L, Wagner N, Gonsiorek W, Hipkin RW, Chou CC, Pugliese-Sivo C, Xiao Y, Tagat JR, Cox K, Priestley T, Sorota S, Huang W, Hirsch M, Reyes GR and Baroudy BM (2005) Discovery and characterization of vicriviroc (SCH 417690), a CCR5 antagonist with potent activity against human immunodeficiency virus type 1. *Antimicrob Agents Chemother* **49**:4911-9.

Tagat JR, McCombie SW, Nazareno D, Labroli MA, Xiao Y, Steensma RW, Strizki JM, Baroudy BM, Cox K, Lachowicz J, Varty G and Watkins R (2004) Piperazine-based CCR5 antagonists as HIV-1 inhibitors. IV. Discovery of 1-[(4,6-dimethyl-5-pyrimidinyl)carbonyl]- 4-[4-[2-methoxy-1(R)-4-(trifluoromethyl)phenyl]ethyl-3(S)-methyl-1-piperaz inyl]- 4-methylpiperidine (Sch-417690/Sch-D), a potent, highly selective, and orally bioavailable CCR5 antagonist. *J Med Chem* **47**:2405-8.

Thompson JD, Higgins DG and Gibson TJ (1994) CLUSTAL W: improving the sensitivity of progressive multiple sequence alignment through sequence weighting, position-specific gap penalties and weight matrix choice. *Nucleic Acids Res* **22**:4673-80.

Tsamis F, Gavrilov S, Kajumo F, Seibert C, Kuhmann S, Ketas T, Trkola A, Palani A, Clader JW, Tagat JR, McCombie S, Baroudy B, Moore JP, Sakmar TP and Dragic T (2003) Analysis of the mechanism by which the small-molecule CCR5

antagonists SCH-351125 and SCH-350581 inhibit human immunodeficiency virus type 1 entry. *J Virol* **77**:5201-8.

Watson C, Jenkinson S, Kazmierski W and Kenakin T (2005) The CCR5 receptor-based mechanism of action of 873140, a potent allosteric noncompetitive HIV entry inhibitor. *Mol Pharmacol* **67**:1268-82.

Westby M, Smith-Burchnell C, Mori J, Lewis M, Mosley M, Stockdale M, Dorr P, Ciaramella G and Perros M (2007) Reduced maximal inhibition in phenotypic susceptibility assays indicates that viral strains resistant to the CCR5 antagonist maraviroc utilize inhibitor-bound receptor for entry. *J Virol* **81**:2359-71.

Wood A and Armour D (2005) The discovery of the CCR5 receptor antagonist, UK-427,857, a new agent for the treatment of HIV infection and AIDS. *Prog Med Chem* **43**:239-71.

Molecular Pharmacology Fast Forward. Published on December 20, 2007 as DOI: 10.1124/mol.107.042101
This article has not been copyedited and formatted. The final version may differ from this version.

FIGURE LEGENDS

Fig. 1. The chemical structures of the five CCR5 antagonists Aplaviroc (APL), Maraviroc (MVC), Vicriviroc (VVC), TAK-779 and TAK-220.

Fig. 2. The sequence alignment of CCR5 with Rhodopsin (1F88). The residues are colored according to their nature. The residues K, R, H are shown in blue; E, D in red; C in green; T, S, Q, N in pink and the rest in black. The TM helices are highlighted and labeled. The automatically generated sequence alignments are manually adjusted to make sure the highly conserved residues on TMs are aligned for homology model building.

Fig. 3. Representative inhibition curves of CCR5 antagonists on ligand binding. Panels **A** and **B** show the dose-dependent percent inhibition of the binding of ^{125}I-labeled chemokine ligands RANTES, MIP1α and MIP1β by VVC and APL, respectively. Binding of all ligands to CCR5 were completely inhibited by these two small molecule antagonists, with the exception that RANTES binding was only partially inhibited by antagonist APL (**B**). Panels **C** and **D** show the dose response curves of the five CCR5 antagonists VVC, MVC, APL, TAK-220 and TAK779 on RANTES binding to the wild-type and E283A mutant CCR5, respectively. The inhibition potency of all antagonists except TAK-779 on the binding of RANTES to E283A mutant CCR5 was significantly reduced (**D**).

Fig. 4. The putative binding pocket is defined after the homology model was built. The key residues (W86, Y108, F109, T195, I198, W248, Y251, E283 and M287) that line the binding pocket are identified and labeled. The TM helices are colored red and labeled from I to VII.

Molecular Pharmacology Fast Forward. Published on December 20, 2007 as DOI: 10.1124/mol.107.042101
This article has not been copyedited and formatted. The final version may differ from this version.

Fig. 5. The shape and electrostatic nature of the five CCR5 antagonists MVC, VVC, APL, TAK-779 and TAK-220. The electrostatic molecular grid that lines molecular volume is colored according to the active lone pair formalism as implemented in MOE software. The green color indicates the hydrophobic parts of the molecule, pink areas indicate the polar areas and electropositive aromatic hydrogens are colored blue. The binding pocket in CCR5 can accommodate antagonists with different shape and electrostatic nature.

Fig. 6. The binding mode for APL (pink). The key salt bridge interaction with E283 is indicated with red dotted lines. APL is predicted to have strong interactions with W86, E283, F109, T195 and I198 (shown in bold). The H-bond with T195 is indicated by black dotted line. The cyclohexyl group of APL is located in a pocket formed by I198, T15 and F109. The seven TM helices are labeled and shown in cyan.

Fig. 7. The binding mode for MVC (orange). The key salt bridge interaction with E283 is indicated with red dotted lines. MVC is predicted to have strong interactions with W86, E283, Y108, Y251 and I198 (shown in bold). The seven TM helices are labeled and shown in cyan.

Fig. 8. The binding mode for VVC (brown), the key salt bridge interaction with E283 is indicated with red dotted lines. VVC is predicted to have strong interactions with W86, E283, Y108, Y251 and I198 (shown in bold). The seven TM helices are labeled and shown in cyan.

Fig. 9. The binding mode for TAK-779 (pink), the key salt bridge interaction with E283 is indicated with red dotted lines. TAK-779 is predicted to have strong interactions with W86, E283, F109, W248, Y251 and I198 (shown in bold). The seven TM helices are labeled and shown in cyan. TAK-779 is the only CCR5 antagonist that interacts strongly with W248. The

phenyl group of TAK-779 points towards TM4. The Y108 residue does not interact with TAK-779.

Fig. 10. The binding mode for TAK-220 (purple), the key salt bridge interaction with E283 is indicated with red dotted lines. TAK-220 is predicted to have strong interactions with E283 and I198 (shown in bold). The seven TM helices are labeled and shown in cyan. TAK-220 is a flexible CCR5 antagonist and it showed minimal reduction in binding affinity to CCR5 carrying certain single amino acid mutations.

Molecular Pharmacology Fast Forward. Published on December 20, 2007 as DOI: 10.1124/mol.107.042101
This article has not been copyedited and formatted. The final version may differ from this version.

Table 1. IC50 values of CCR5 antagonists in inhibiting ligand binding and HIV-cell fusion*

	Ligand binding assay			CCF assay	Antiviral assay
	^{125}I-RANTES	^{125}I-MIP-1α	^{125}I-MIP-1β		
Ligand Kd (nM)**	0.59±0.1	1.4±0.5	0.4±0.5		
Vicriviroc	14±1	11±8	12±3	1.2±0.4	7.2±2
Maraviroc	9± 9	4±1	3±1	1.2±0.5	1.4±1
TAK779	4±5	7.5±5	4.5±1	18±2	13±6
TAK 220	17±5	7±1	4,100±320	6.1±4	3±4
Aplaviroc	12±2	8.5±3	7.3±0.2	1±0.6	1±1

* Data are mean and standard errors in mM; data were derived from three independent experiments.

** Kd values are for various ligands binding to the WT CCR5

Molecular Pharmacology Fast Forward. Published on December 20, 2007 as DOI: 10.1124/mol.107.042101
This article has not been copyedited and formatted. The final version may differ from this version.

Table 2. IC50 values (μM) of CCR5 antagonists in inhibiting RANTES binding to WT and mutant CCR5

	WT	T195A	I198A	W86A	W94A	Y108A	F109A	W248A	Y251A	E283A	M287A
CCR5 expression*	100 ± 8.4	71.1 ± 6.8	78.1 ± 11.1	55 ± 4.9	119 ± 12.4	89 ± 7.5	59.8 ± 6.7	98.7 ± 8.8	63.7 ± 7.3	87.5 ± 9.1	112.2 ± 11.7
RANTES Kd	0.0006 ± 0.0001	0.0007 ± 0.0002	0.0004 ± 0.0001	0.003 ± 0.0004	UD**	UD	0.006 ± 0.0005	0.0006 ± 0.0002	0.0002 ± 0.0001	0.013 ± 0.002	0.001 ± 0.0003
Vicriviroc	0.014 ± 0.001	0.022 ± 0.006	0.35 ± 0.007	0.091 ± 0.01	0.03 ± 0.007	0.84 ± 0.016	0.026 ± 0.009	0.02 ± 0.002	0.255 ± 0.03	9.8 ± 1.6	0.055 ± 0.03
Maraviroc	0.009 ± 0.0008	0.014 ± 0.01	0.81 ± 0.07	0.09 ± 0.05	0.01 ± 0.01	0.63 ± 0.16	0.0079 ± 0.001	0.013 ± 0.013	0.113 ± 0.066	18 ± 4	0.0033 ± 0.0004
TAK-779	0.004 ± 0.001	0.02 ± 0.005	0.026 ± 0.006	0.211 ± 0.05	0.011 ± 0.003	0.113 ± 0.034	0.009 ± 0.003	0.028 ± 0.008	0.011 ± 0.003	0.043 ± 0.009	0.005 ± 0.001
TAK 220	0.017 ± 0.003	0.005 ± 0.001	0.932 ± 0.221	0.03 ± 0.008	0.024 ± 0.005	0.012 ± 0.002	0.005 ± 0.001	0.004 ± 0.001	0.011 ± 0.003	11.0 ± 1.4	0.029 ± 0.006
Aplaviroc	0.01 ± 0.002	0.122 ± 0.045	0.354 ± 0.07	0.387 ± 0.04	0.033 ± 0.008	0.057 ± 0.011	1.577 ± 0.214	0.007 ± 0.002	0.025 ± 0.005	0.603 ± 0.084	0.066 ± 0.015

* Expression level of mutant CCR5 relative to the wild-type CCR5

** Undeterminable

Molecular Pharmacology Fast Forward. Published on December 20, 2007 as DOI: 10.1124/mol.107.042101
This article has not been copyedited and formatted. The final version may differ from this version.

Table 3. Fold change of IC50 values*

	WT	T195A	I198A	W86A	W94A	Y108A	F109A	W248A	Y251A	E283A	M287A
Vicriviroc	1	1.6	25	6.5	0.8	60	1.9	1.4	18.2	700	1.6
Maraviroc	1	1.6	89	10	2.0	70	0.9	1.4	12.2	2000	0.4
TAK-779	1	5.0	6.5	53	2.8	28	2.3	7.0	2.8	11	1.3
TAK-220	1	0.3	55	1.8	1.4	0.7	0.3	0.2	0.6	647	1.7
Aplaviroc	1	12.2	35	39	3.3	5.7	158	0.7	2.5	61	6.6

* Fold changes of IC50 values for CCR5 antagonists in inhibiting RANTES binding to mutant CCR5 by comparing to binding to the WT CCR5

Molecular Pharmacology Fast Forward. Published on December 20, 2007 as DOI: 10.1124/mol.107.042101
This article has not been copyedited and formatted. The final version may differ from this version.

Figure 1.

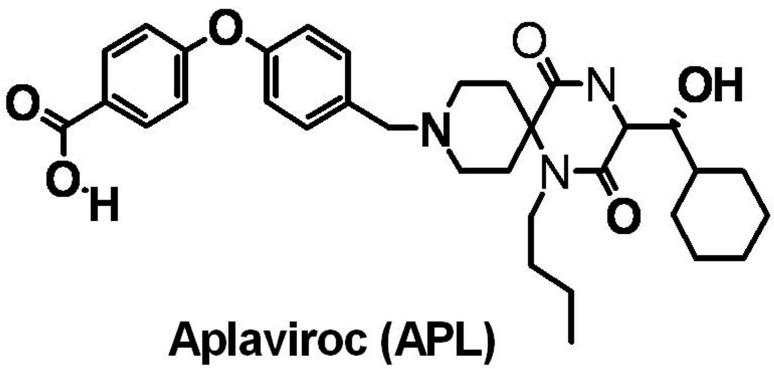

Aplaviroc (APL)

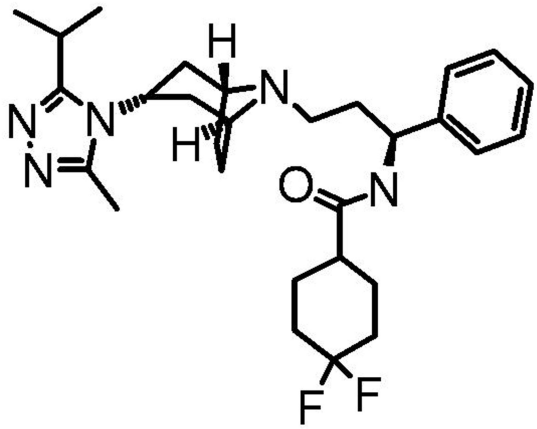

Maraviroc (MVC)

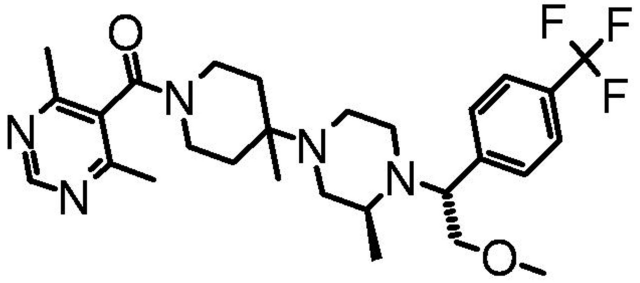

Vicriviroc (VVC)

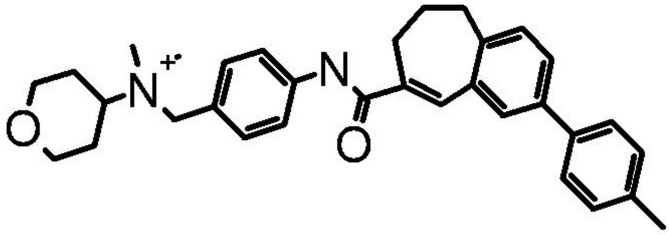

TAK-779

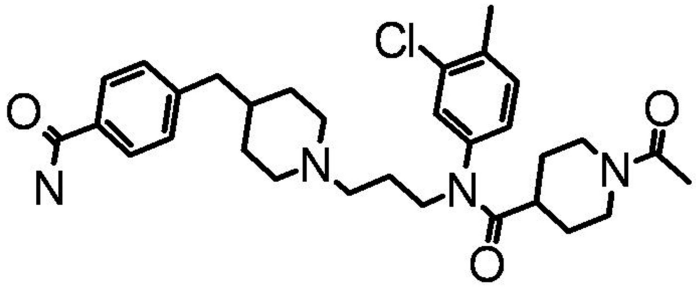

TAK-220

Figure 2.

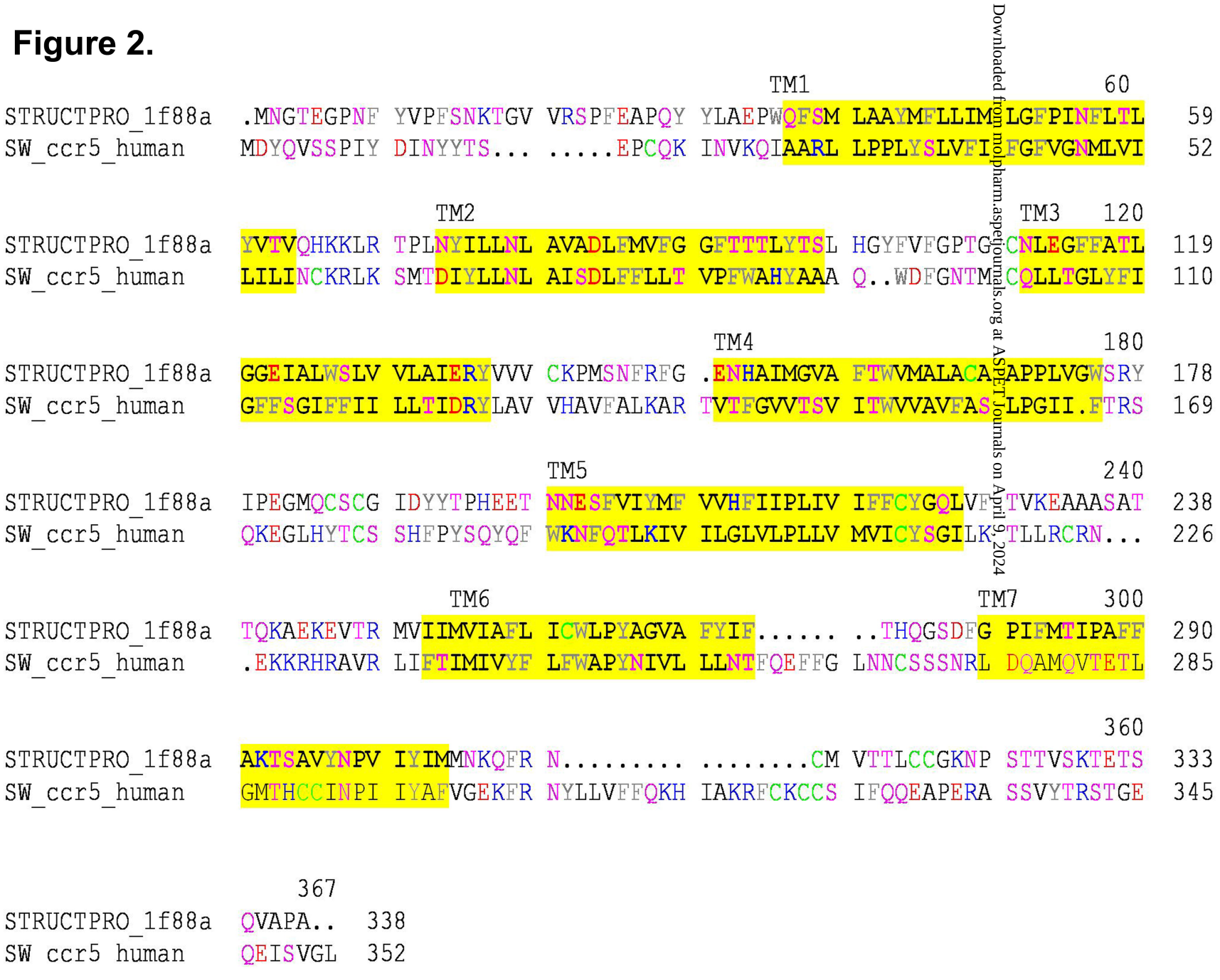

Figure 3.

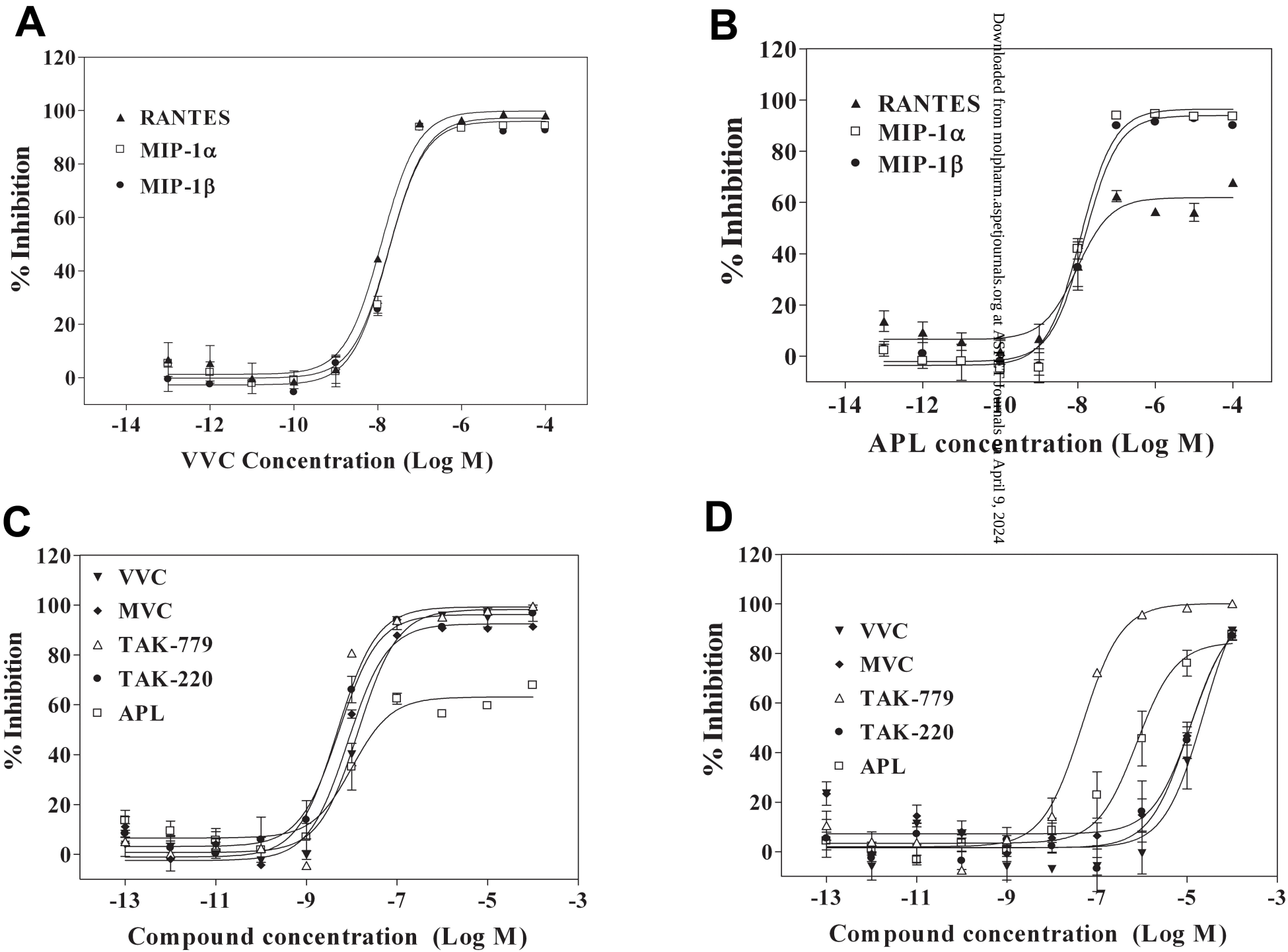

Figure 4.

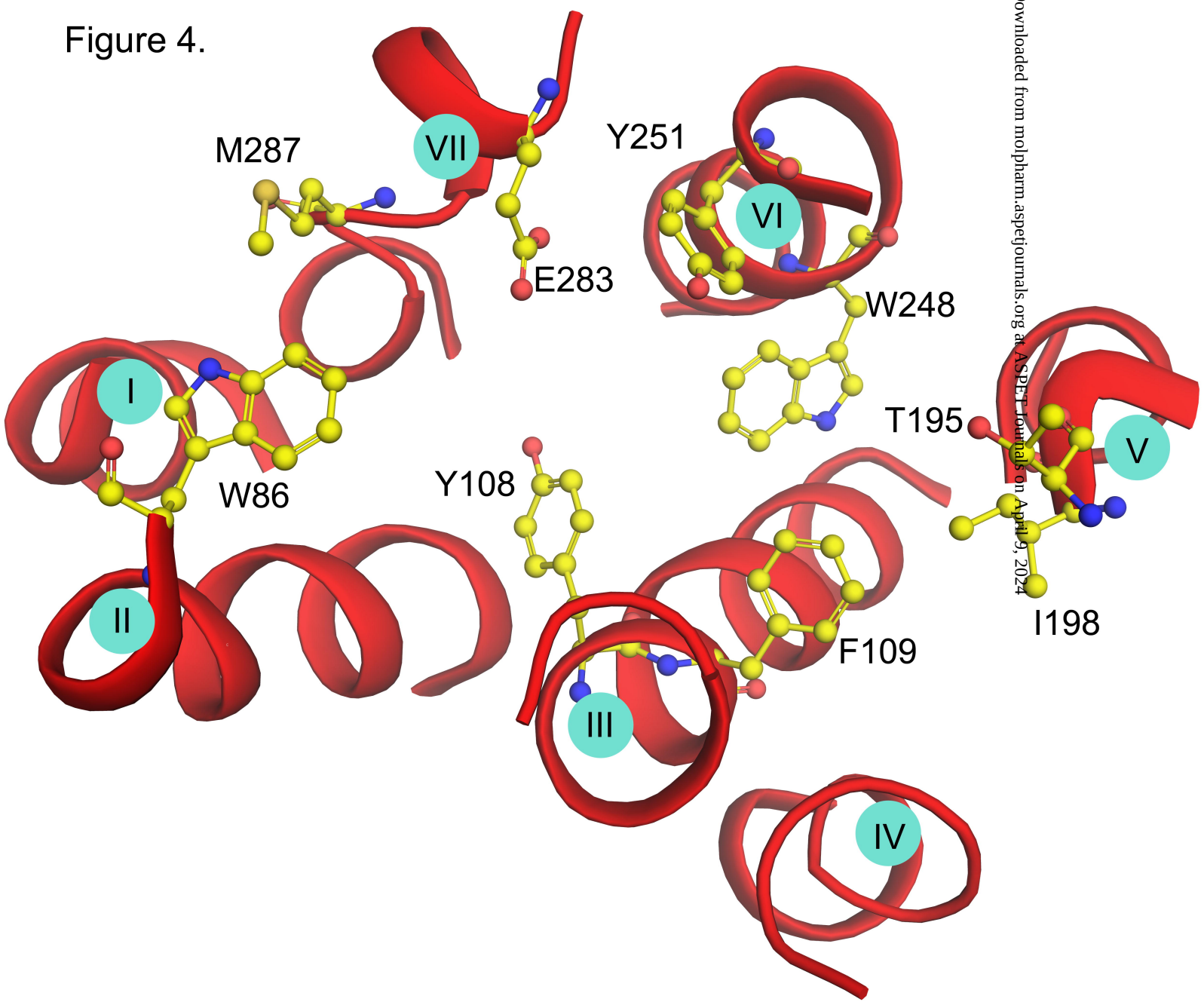

Figure 5.

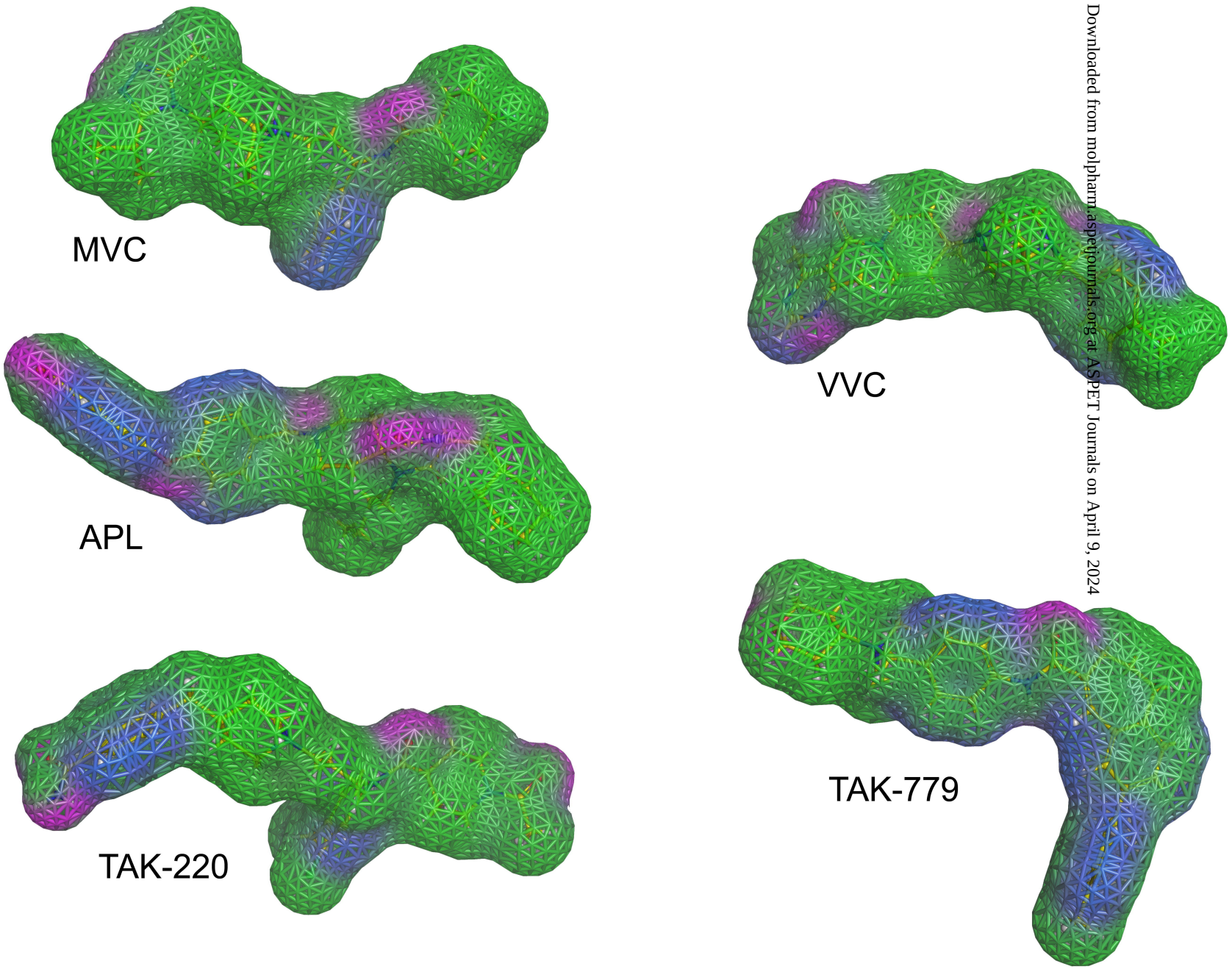

Figure 6.

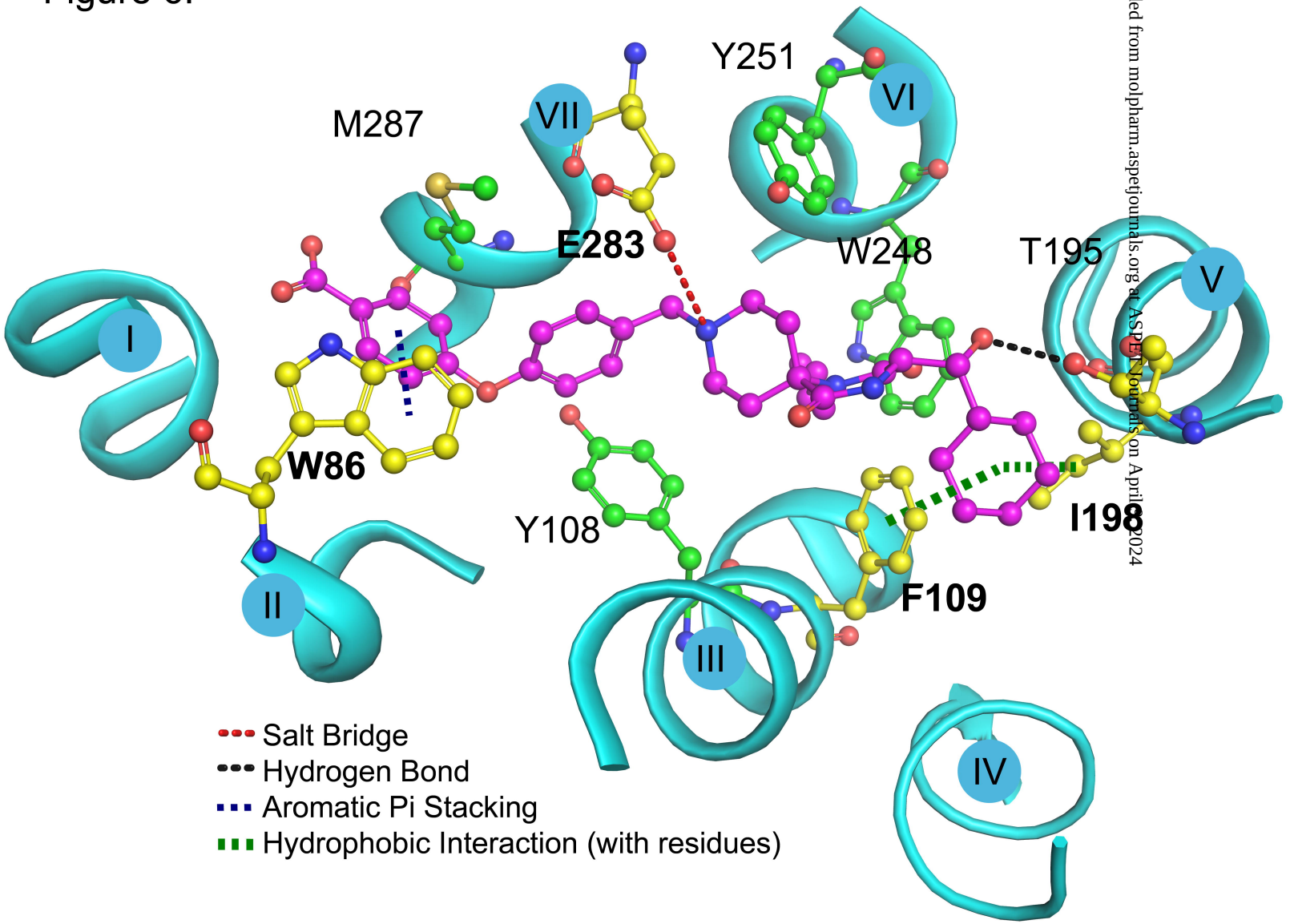

Figure 7.

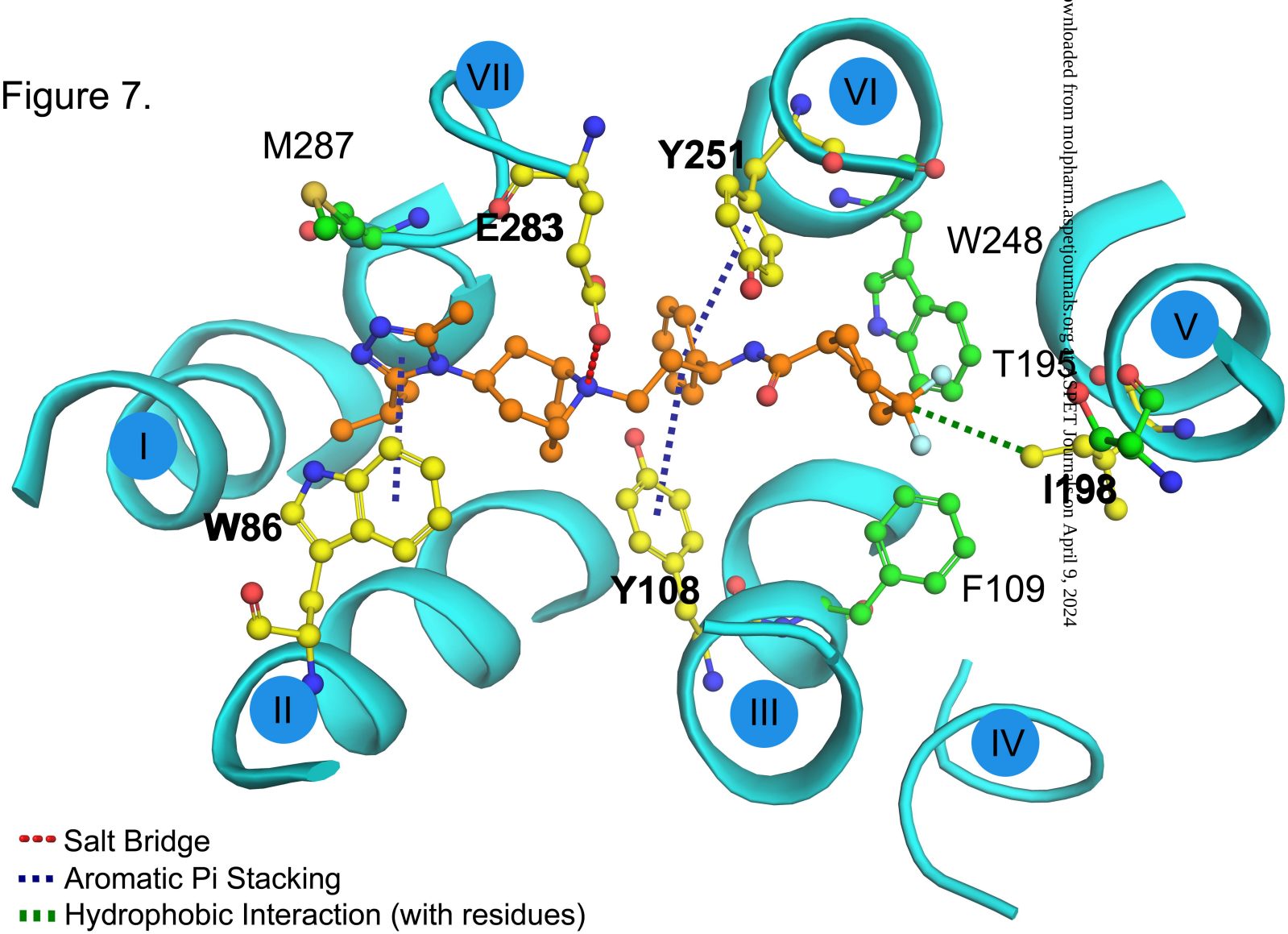

Figure 8.

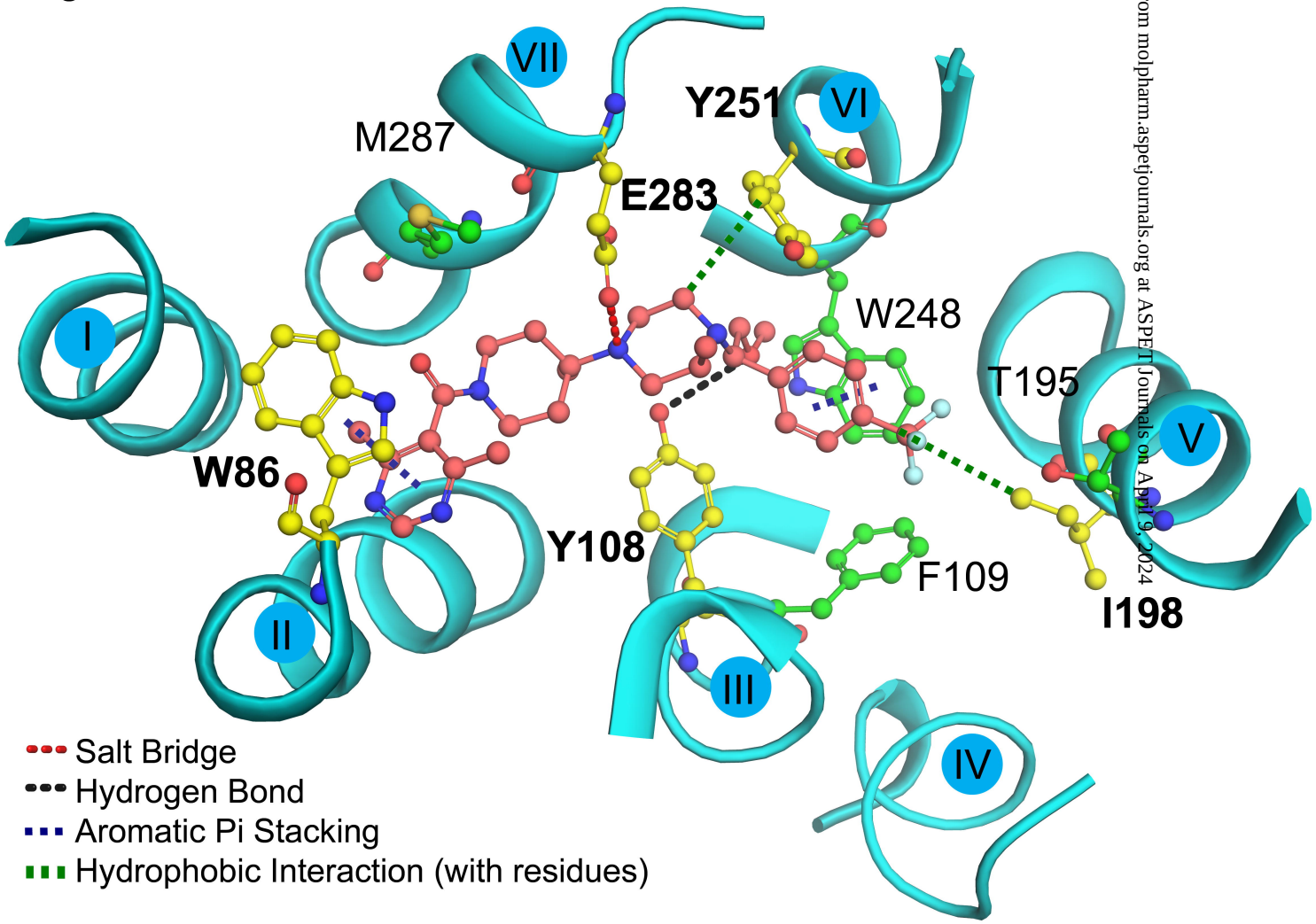

Figure 9.

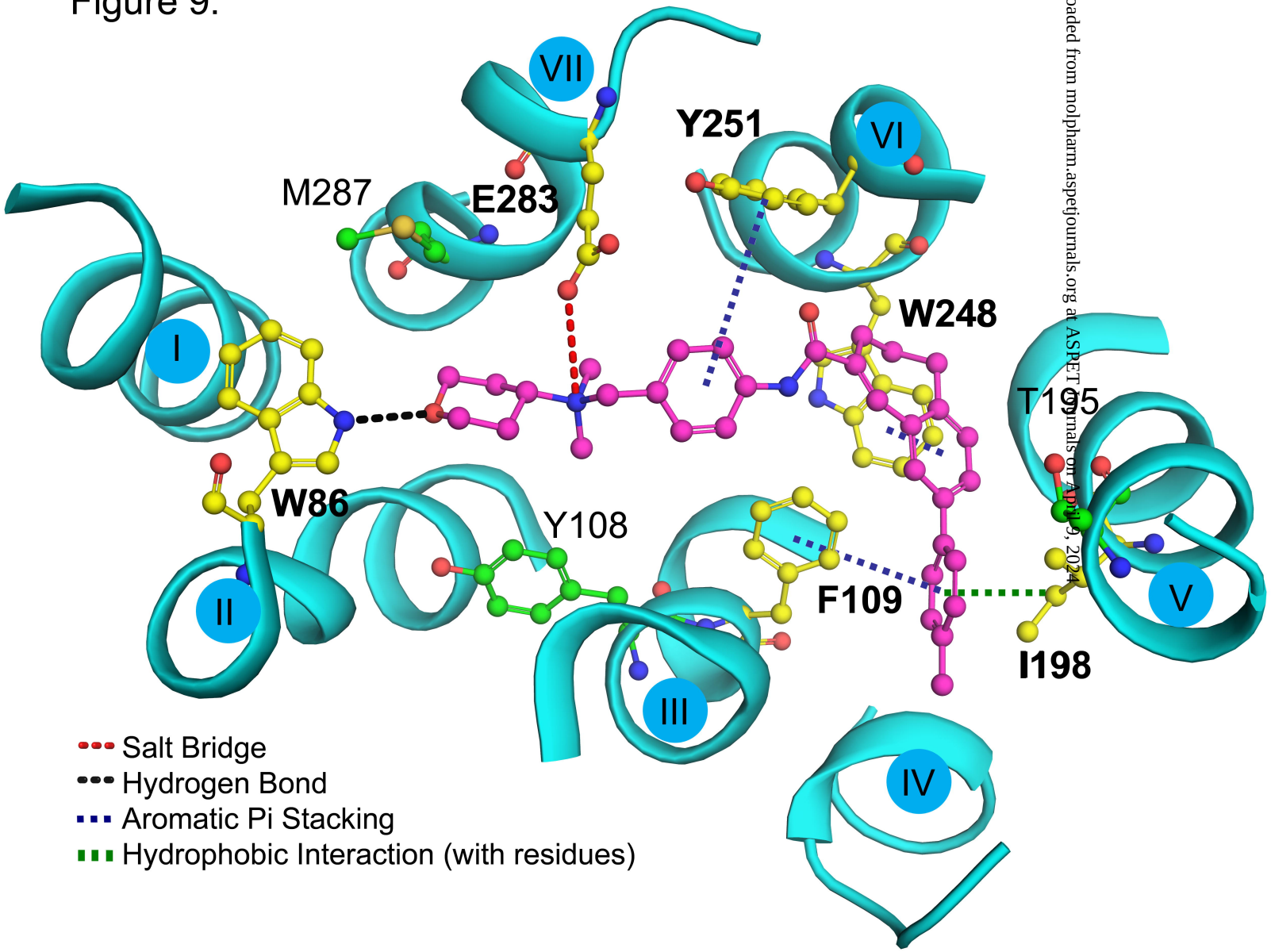

Figure 10.